Molecular Crystals and Liquid Crystals Science and Technology. Section A. Molecular Crystals and Liquid Crystals

Publication details, including instructions for authors and subscription information:
http://www.tandfonline.com/loi/gmcl19

Transverse Patterns in Optical Reorientation of Nematic Liquid Crystals with a Single Feedback Mirror

R. Macdonald [a] & H. Danlewski [a]

[a] Optisches Institut Technische Universität, Berlin Strasse des 17. Juni 135, D-10623, Berlin, Germany

Version of record first published: 24 Sep 2006.

To cite this article: R. Macdonald & H. Danlewski (1994): Transverse Patterns in Optical Reorientation of Nematic Liquid Crystals with a Single Feedback Mirror, Molecular Crystals and Liquid Crystals Science and Technology. Section A. Molecular Crystals and Liquid Crystals, 251:1, 145-158

To link to this article: http://dx.doi.org/10.1080/10587259408027199

Mol. Cryst. Liq. Cryst. 1994, Vol. 251, pp. 145–158
Reprints available directly from the publisher
Photocopying permitted by license only

Printed in the United States of America

TRANSVERSE PATTERNS IN OPTICAL REORIENTATION OF NEMATIC LIQUID CRYSTALS WITH A SINGLE FEEDBACK MIRROR

R. Macdonald and H. Danlewski
Optisches Institut Technische Universität Berlin
Strasse des 17. Juni 135, D-10623 Berlin, Germany

Abstract. Spontaneous transverse pattern formation is investigated in optical reorientation of nematic liquid crystals with a single feedback mirror experiment. The influence of the distance between the optically nonlinear nematic film and the mirror, the input beam symmetry and intensity upon the patterns is shown.

INTRODUCTION

Complex transverse effects in nonlinear optics like spontaneous pattern formation and nonlinear dynamic phenomena have attracted increasing interest during the recent years [1, 2]. One motivation for this interest may be that these problems are of basic interest for many different disciplines of modern science and that optical systems allow reproducible experiments with established methods under well defined boundary conditions. Furthermore, the well developped concept of nonlinear optics in addition to the Maxwell theory can be used for theoretical description.

Secondly, nonlinear dynamics and pattern formation may inherently appear in many nonlinear optical devices like e.g. optically bistable filters [3] or lasers [4] leading to complex spatial and temporal behaviour. Pattern formation and self-organization is also discussed to be important in future applications like optical pattern recognition [5] and assosiative memory [6] or optical information storages [7].

In order to understand features of pattern formation processes in more complex systems, one needs to deal with simpler systems first. Recently, a rather simple arrangement, consisting of a thin Kerr-slice in front of a single feedback mirror was discussed theoretically [8] to exhibit spontaneous two-dimensional pattern formation, which was experimentally verified [9] short after and proved later on [10] using a nematic liquid crystal as nonlinear optical media.

In the present paper the influence of experimental parameters like the distance between the nonlinear film and the feedback mirror, the intensity and the symmetry of the finite diameter input laser beam upon the patterns is shown. Experimental observations are theoretically discussed performing a linear stability analysis of the single feedback mirror arrangement.

EXPERIMENTAL SETUP

The experimental setup as shown in Fig.1 and the principles of optical pattern formation for this arrangement have been described in detail previously [9, 10] and will only be briefly reviewed here. Consider a homeotropically or hybridly aligned nematic liquid crystal film 5CB (pentyl-cyanobiphenyl) of 100 μm thickness, stacked between two glass plates and placed several centimeters in front of a plane high reflectivity mirror R = 0.98. The birefringent optically nonlinear liquid crystal is illuminated with a 2 mm diameter TEM_{oo} mode cw argon ion laser beam of wavelength $\lambda = 514$ nm which is linearly (extraordinary) polarized. To avoid on-axis reflections at the glass surfaces the sample is tilted to Brewster's angle unless not noted otherwise.

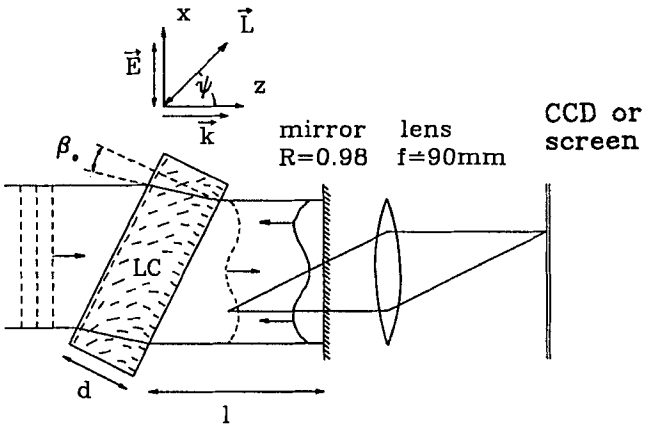

Fig. 1: Experimental setup of the feedback mirror arrangement. A hybridly or homeotropically (not shown here) aligned liquid crystal (LC) is placed in front of a high reflectivity mirror and illuminated with a linear polarized cw laser beam. ***E*** is the optical field, ***k*** the light wave-vector and ***L*** the nematic director.

Generally, the transmitted beam behind the liquid crystal film contains a small phase modulation which results e.g. from spontaneous fluctuations in molecular alignment and hence fluctuations in birefringence. The phase modulated beam then propagates to the mirror and back, reentering the film as an amplitude modulated beam. The change from phase to amplitude modulation is due to the free space light propagation. The returning amplitude modulation is then again changed into phase modulation as a result [9,10] of the reorientational optical nonlinearity thus closing the feedback loop. The pattern formation can be understood in terms of Talbot-plane assisted instabilities of certain spatial modes (i.e. "optical gratings") of the above mentioned spontaneous fluctuations. Since these kind of instabilities are connected with transverse diffraction effects they will be called *diffractive* pattern formation in contrast to the wavelenght scaled counterpropagating instabilities which may additionally occur e.g. in resonators under the conditions of optical bistability.

The resulting patterns have been investigated by imaging the near field distribution behind the film on a screen or a CCD-camera, respectively, with the help of a lens through the remaining 2% transmission of the feedback mirror.

MATHEMATICAL DESCRIPTION AND LINEAR STABILITY ANALYSIS

Theoretically the system can be treated using an equation for the optical reorientation and thus the light-induced phase modulation inside the liquid crystal in addition to Maxwell equations describing the light propagation. The diffusion limited reorientational optical nonlinearity can be described in the small angle approximation by a modulation in the extraordinary refractive index $n = n_{eq} + \bar{n}$ where $\bar{n} = \bar{n}_o \sin\{\pi z/d\}$ and the index change at $z = d/2$ is determined by [11]

$$\tau_r \partial_t \bar{n}_o - \xi^2 \nabla_\perp^2 \bar{n}_o + \bar{n}_o = \frac{1}{2} \varkappa \tilde{E}^2 \qquad (1)$$

with $$\xi^2 = \frac{K}{\varepsilon_o \varepsilon_a (E_{fred}^2 - E^2 (1 - \sin 2\beta))} \quad \text{and} \quad \tau_r = \xi^2 \frac{\gamma_1}{K}$$

where $\partial_t = \partial/\partial t$. $\tilde{E}^2 = (E / E_{fred})^2$ is the reduced intensity with respect to the Freedericks intensity $E_{fred}^2 = \pi^2 K/(d^2 \varepsilon_o \varepsilon_a)$ and $\varkappa = \sin\{2\beta\} \varepsilon_a n_\perp/(4 n_\parallel^2)$ in case of homeotropic alignment. For hybridly aligned samples $\varkappa$ has a somewhat

different value, see ref. 9. The 5CB liquid crystal parameters are (at $T = 300\,K$) the elastic constant $K = 6 \cdot 10^{-12}\,N$ (in a one constant approximation), the viscosity $\gamma_1 = 0.08\,kg/m\,s$, the principal refractive indizes $n_\perp = 1.54$, $n_\parallel = 1.73$ and the optical anisotropy $\varepsilon_a = 0.62$. The angle between the beam propagation and the initial optical axis inside the tilted film is denoted with β ($= 33.5$ deg). Since the intensities needed for pattern formation are generally much smaller than the Freedericks intensity [9] we will assume a constant diffusion length $\xi = 30\,\mu m$ and relaxation time $\tau_r = 12\,s$ in the following, using the above parameters.

The intentsity E^2 on the right hand side of eq. 3 consist of the forward input intensity E_{in}^2 and the transmitted backward intensity E_b^2, returning from the mirror and can be calculated by the Maxwell equations which hold in the slowly-varying envelope (SVE) approximation as

$$\partial_z E = i k n_{eq} \bar{n} E \qquad \text{for } -d \le z \le 0 \tag{2}$$

$$\partial_z E = \frac{i}{2k} \nabla_\perp^2 E \qquad \text{for } 0 \le z \tag{3}$$

where $\partial_z = \partial/\partial z$ and $k = 2\pi/\lambda$. In writing eqns. 1 to 3 it has been assumed that the light beam propagates along the z-axis and that the effective sample thickness is d. According to eq. 2 the transmitted amplitude is phase modulated immediatly behind the nonlinear film and can be used as an input for the propagator eq. 3 which is then formally integrated to give the returning backward amplitude [12]

$$E_b = \sqrt{R}\, \exp\{\frac{i\,l}{k} \nabla_\perp^2\} \left(E_{in} \exp\{\frac{i\,2k\,n_{eq}\,d}{\pi} n_o \} \right) \tag{4}$$

Note that generally the operator $\exp\{il/k\, \nabla_\perp^2\} = 1 + il/k\, \nabla_\perp^2 + \frac{1}{2}(il/k\, \nabla_\perp^2)^2 + \ldots$. has to be applied on both the (smoothly) spatially varying amplitude E_{in} and the phase $\exp\{i\,2k\,n_{eq}\,d\,\bar{n}_o/\pi\}$ in case of Gaussian laser beams. The total intensity at the liquid crystalline film can then be written as

$$E^2 = E_{in}^2 + R \left| \exp\{\frac{i\,l}{k} \nabla_\perp^2\} \left(E_{in} \exp\{\frac{i\,2k\,n_{eq}\,d}{\pi} \bar{n}_o \}\right)\right|^2 \tag{5}$$

where we have assumed that wavelength scaled gratings of counterpropagating beams can be neglected because of the large diffusion constant ξ. We will

further neglect the temporal delay between the actual refractive index change and the returning amplitude modulation which is determined by the round trip time for the light propagation from the nonlinear film to the mirror and back, since the relaxation time τ_r of the liquid crystal is several orders of magnitude larger.

Using the intensity eq.5 as a source in eq. 1, the first term causes a smoothly varying phase modulation because of the input beam intensity profile but does not contribute to the pattern formation process. It will be omitted therefore in the following. With the second term a generalized Ginzburg-Landau equation[13] is obtained for the description of the nonlinear system. A linear and nonlinear stability analysis of such a system has been performed in Ref. 12 in the approximation of plane electromagnetic input waves. It was shown that hexagonal spatial patterns are expected to appear. We will drop here the plane wave approximation and consider the influence of the finite diameter input beam on the patterns in a first attempt by simply assuming

$$E_{in} = \begin{cases} E_{in}^2 = \text{const.} & \text{for } 0 \le \rho \le w_o \\ 0 & \text{for } \rho > w_o \end{cases} \qquad (6)$$

where w_o denotes the beam radius. As a result the intensity E_{in}^2 can be commuted through the operator in the source eq. 5 for $\rho \le w_o$ and a homogeneous eq. 1 is obtained for $\rho > w_o$. The spatial modes and patterns of the system will be discussed analytical performing a linear stability analysis. Using the first term in a Taylor series expansion of the phase factor in eq. 5 the linearized equation can be written as

$$\tau_r \partial_t \bar{n}_o - \xi^2 \nabla_\perp^2 \bar{n}_o + \bar{n}_o = -2\tilde{\varkappa} R \tilde{E}_{in}^2 \sin\{\frac{1}{k} \nabla_\perp^2\} \bar{n}_o \qquad (7)$$

where $\tilde{\varkappa} = 2 k n_{eq} d \varkappa/\pi$. The spatial modes can be found by solving the wave equation

$$\nabla_\perp^2 \bar{n}_o = - q^2 \bar{n}_o \qquad (8)$$

with respect to additional boundary conditions. Solutions may be e.g. harmonic functions (then q is the pattern wavenumber), Besselfunctions or spherical harmonic functions. In our case it is appropriate to use cylindrical transverse coordinates (ρ, φ) and $\nabla_\perp^2 = \rho^{-1} \partial_\rho (\rho \partial_\rho) + \rho^{-2} \partial_\varphi^2$ because of the cylindrical sym-

metry of the input laser beam around the z-axis. Solutions of eq. 7 with respect to the boundary conditions eq. 6 and $\bar{n}_o(\rho \to \infty) = 0$ can then be written [14]

$$\bar{n}_o = \begin{cases} \bar{n}_m(q,t)\ \cos\{m\varphi\}\ J_m(q\rho) & \text{for } 0 \le \rho \le w_o \\ \bar{n}'_m(\xi,t)\ \cos\{m\varphi\}\ K_m(\rho/\xi) & \text{for } \rho > w_o \end{cases} \tag{9}$$

where J_m and K_m are Besselfunctions, respectively modified Besselfunctions of first kind and integer order m. Continuity of the solutions eq. 9 and their derivatives at $\rho = w_o$ yields the additional boundary condition [15]

$$q\xi = \frac{\partial_\rho K_m(w_o/\xi)\ J_m(q\,w_o)}{K_m(w_o/\xi)\ \partial_\rho J_m(q\,w_o)} \tag{10}$$

which for every integer m defines a discrete spectrum of q-values for a given diffusion length ξ and beam radius w_o.

To discuss the stability of the patterns the cylindrical modes eq. 9 using the discrete values q determined from eq. 10 are put into eq. 7 which yields for the dynamics of the amplitudes

$$\bar{n}(t) \sim \exp\{-t/\tau\} \tag{11}$$

where

$$\tau = \frac{\tau_r}{1 + \xi^2 q^2 - 2\tilde{\varkappa} R \tilde{E}_{in}^2 \sin\{\vartheta\}} \tag{12}$$

and $\vartheta = l k^{-1} q^2$ is the phase difference between the unpertubed and the diffracted wave behind the film. In Fig. 2 we have plotted τ_r/τ as a function of ϑ using eq. 12. Modes with $\tau^{-1} > 0$ are stable and decay exponentially according to eq. 11 whereas $\tau^{-1} < 0$ defines instable patterns, growing exponentially above a certain threshold intensity $(E_{th})^2$ which is determined from $\tau^{-1} = 0$. At low intensities $E^2 < (E_{th})^2$ the relaxation rate τ^{-1} is positive for any q and the homogeneous solution of eq. 7 is prominent. With increasing intensity the mode(s) having lowest threshold become instable and appear as a pattern. These are generally the modes which are at or close to the absolute minimum threshold $(E_{th}^{min})^2$ which is determined (for a given diffusion constant ξ) by

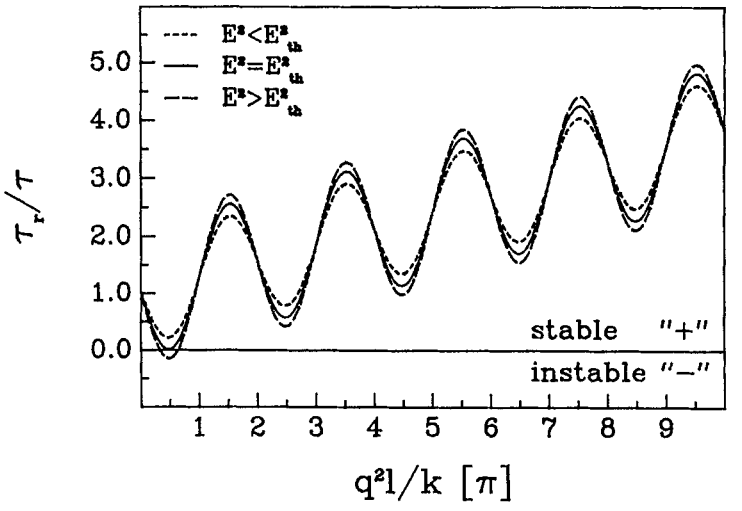

Fig. 2: Relaxation rate τ_r/τ for pattern formation as a function of ϑ for three different input intensities E^2.

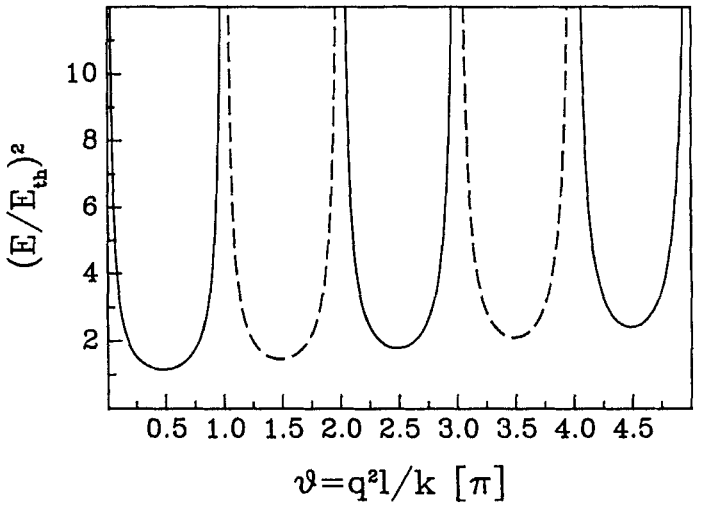

Fig. 3: Threshold intensity as a function of ϑ. Solid line corresponds to positive ($\varkappa > 0$), dashed line to negative ($\varkappa < 0$) optical nonlinearity.

the phase ϑ as shown in Fig. 3. Using the experimental parameters given above the minimum threshold is given in our case by $\vartheta_{min} = \pi/2$ which leads to [8, 9]

$$q_{min} = \pi \, (\lambda l)^{-1/2} \tag{13}$$

It was shown [12] that for plane input waves the instable modes and the expected patterns close to threshold are hexagons with the wavenumber q_{min} which is determined for a given laser wavelength by the distance l. This is, however, not necessarily the case with finite diameter laser beams since only certain values of q are allowed according to additional boundary conditions, cf. eq. 10. Secondly, for the cylindrical modes eq. 9 the integer m determines the symmetry and the appearence of the patterns rather than q as will be shown below. The allowed values q and the order m of the Besselfunctions are, however, connected to each other via the boundary condition eq. 10. For a given m the belonging values q determine the relaxation rate eq. 12 and thus the instability of the mode(s). In general, the modes m which have q values close to the minimum q_{min} appear since they have lowest threshold.

The influence of the beam diameter upon the observed patterns for a fixed distance l can be understood within the model as follows: Changing w_o will shift the discrete spectrum q given by eq. 10 with respect to the minimum threshold intensity shown in Fig. 3. As a result different modes m are more or less close to this minimum and the closest will appear as the dominant pattern which becomes unstable at lowest intensity.

EXPERIMENTAL RESULTS AND DISCUSSION

Examples of the observed patterns which have been obtained with a hybridly aligned sample are given in Fig. 4 for different distances l. Clearly the characteristic spatial period $\Lambda = q/2\pi$ of the patterns increases with increasing l. Obviously the patterns are no hexagons at all which will be discussed in more detail and with respect to the previous theoretical considerations below. The threshold intensity in these experiments has been measured to range around $I_{th} = 12\,W/cm^2$ with an uncertinity of at least 10%. This is in good agreement with the theoretical value of $9\,W/cm^2$ for $l = 10\,cm$ using the material parameters given above. According to plane wave theory the threshold is expected [8] to exhibit a weak dependence upon the distance l (cf. Fig. 3) which

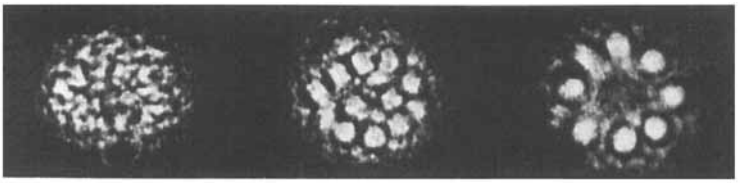

Fig. 4: Spontaneous optical patterns in a hybridly aligned nematic liquid crystal for three distances l between the nonlinear film and the feedback mirror.

was not found within our experimental uncertinity. It has been discussed in Ref. 9 that this may be also established in the fact that finite laser beams have been used instead of plane waves.

In Fig. 5 we have plotted the evaluated wavenumbers of the patterns as a function between the liquid crystal film and the mirror. The experimentally observed wavenumbers q are fairly close to the theoretically expected value q_{min} as given by eq. 13.

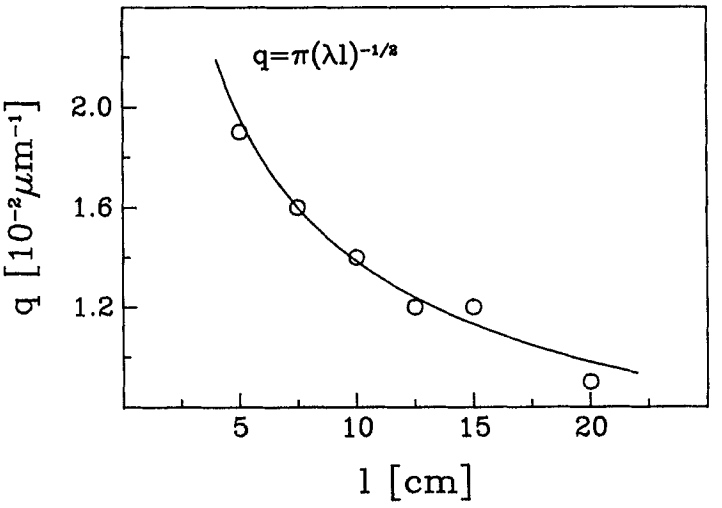

Fig. 5: Evaluated pattern wavenumbers q as a function of the distance l.

In Fig. 6 we have displayed examples of patterns obtained with homeotropic samples which can be described quite well by the above discussed cylindrical

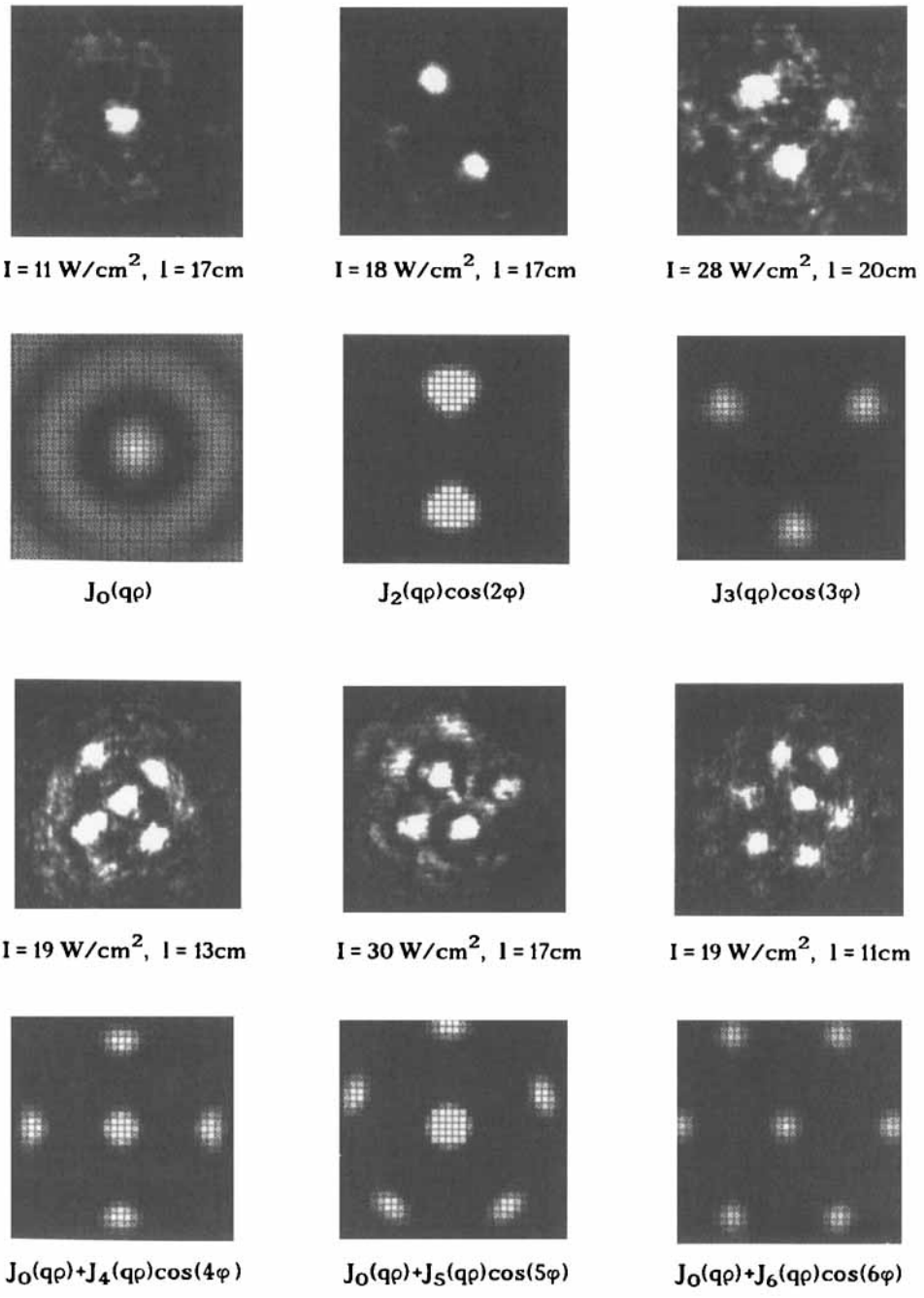

Fig. 6: Examples of patterns obtained with a homeotropic aligned nematic liquid crystal and comparision with calculated cylindrical modes, cf. eqns.9.

modes as shown for comparison. The theoretical patterns have been calculated using the intensity according to eq. 5 for a small distance z behind the film in the approximation of weak phase modulations eq. 9. Different modes m have been realized by changing the distance l between 11 and 20 cm and by changing the input intensity between 10 and 30 W/cm^2. Clearly, patterns with $m = 0$, $m = 2$, $m = 3$ and mixed modes $m = 0$ plus $m = 4$, $m = 5$ or $m = 6$ have been observed. Another example with $m = 8$ was already shown in Fig. 5 for $l = 20$ cm. In these experiments, the first instable mode which usually occured from the smoothly varying ("homogeneous") input intensity profile at lowest threshold (about $I = 10\ W/cm^2$) is $m = 0$, appearing as a bright center spot inside of a ring. Further increasing of the intensity then usually leads to further bifurcations into modes dispalyed above, depending on the distance l and intensity. Combinations of the Besselfunction $m = 0$ with higher order Besselfunctions have been only observed for $4 \leq m \leq 6$ so far. This may be established in the fact that for a given q the second maximum of $J_0(q\rho)$ is (more or less) close to the first maximum of $J_m(q\rho)$ with $m = 4$, 5 and 6 but not for $m = 2$, 3 or 8.

As discussed in the theoretical section the instable modes are e.g. determined by the beam waist w_o on one hand and the distance l on the other hand. Consequently changes in l and the intensity I select different modes m since the effective radius w_o of the beam may be defined as the radius where the intensity is above threshold in case of a Gaussian laser beam profile.

It should be noted that very similiar patterns have been reported recently [16] for numerical simulations of a Kerr-slice in front of a feedback mirror considering Gaussian input intensity profiles. The calculated patterns have been discussed in this reference in the context of O_2 symmetry-breaking of the input beam into patterns with reduced space groups D_m where m is an integer. Our analytically calculated patterns $J_m(q\rho)\cos(m\varphi)$ exactly describe the same symmetry breaking, except for $m = 0$. If we consider the investigated pattern formation processes as phase transitions [13], the latter means that instability of the mode $m = 0$ must be connected with a first order transition whereas the symmetry breaking transitions may be of first *or* second order, in principle, which will be discussed elsewhere.

For rather large beam diameter and/or increased intensities several modes may become instable and the observed patterns are superpositions of many cylindrical modes. Consequently more complex two-dimensional patterns are

observed in these cases, which at least can be called "hexagon-like" but are not exactly hexagons at all.

Finally we will demonstrate that further reduction of the input intensity symmetry may lead to completely different patterns. Fig. 7 displays a quasi one-dimensional near field grating structure together with the corresponding far field distribution observed approximately 2.5 m behind the nonlinear film.

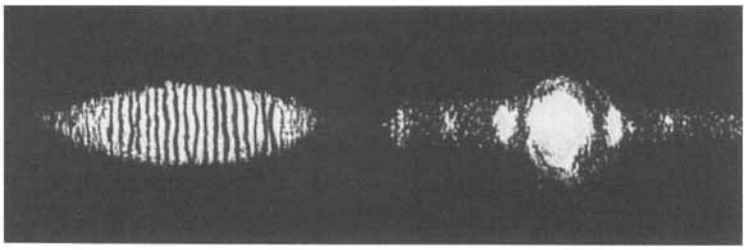

Fig. 7: One-dimensional patterns ("rolls"), obtained with an elliptical intensity profile 2 mm x 0.7 mm and $l = 1$ cm. The spatial period is $\Lambda = 100\,\mu$m.

The pattern has been obtained by focussing the input beam with a cylindrical lens to an elliptical intensity profile of about 2mm x 0.7 mm at the liquid crystal film and placing the mirror at the beam waist. For photographing the far field pattern, the laser beam has been recolimated with another cylindrical lens behind the mirror. The distance between the nonlinear film and the mirror was $l = 1$ cm and the tilt angle was $\beta = 10$ deg. The Fourier component of the grating is clearly present in the far field and the patterns may be called "rolls" in analogy to the hydrodynamic Rayleigh-Bénard instability. The grating period was $\Lambda = 100\,\mu$m in these experiments.

In some cases we observed also a transition from one-dimensional gratings to two-dimensional patterns by increasing the intensity even with axially symmetric input beams as shown in Fig. 8. Since such transitions are not expected from nonlinear stability analysis and numerical simulations of a similiar system [12] (in a plane wave approximation) for any value of the control parameter, it can be assumed that the observed rolls result also from asymmetries in the system which become less important with increasing intensity. The symmetry of the system may be reduced e.g. as a result of the slanted sample, misalignment of the feedback mirror or anisotropic diffusion of the

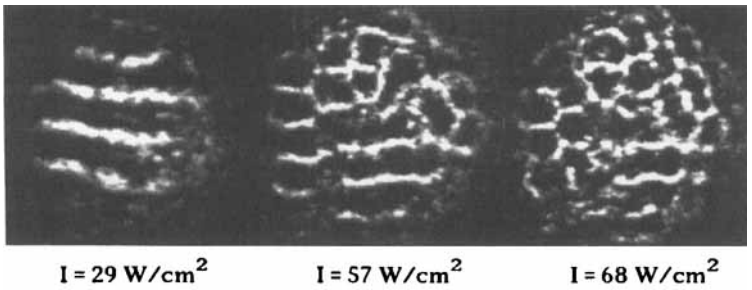

Fig. 8: Transition from rolls to two-dimensional patters by increasing the input intensity for a homeotropic aligned nematic liquid crystal, l = 5.5cm.

nonlinearity. In our experiments the asymmetry and the direction of the grating wave-vector was clearly related to a small misalignment of the feedback mirror, which has been proved by slightly slanting the mirror. The grating wave-vector of the observed rolls was always parallel to the tilt axis. A similiar result can be expected for extremely slanted samples, because the assumption of a constant mirror distance l obviously is no longer valid in this case for the direction perpendicular to the tilt axis, leading to asymmetric feedback.

CONCLUSIONS

Spontaneous transverse pattern formation and diffractive spatial instabilities have been investigated in a single feedback mirror arrangement using a nematic liquid crystal as a nonlinear optical medium. Grating wavenumbers of the patterns and threshold intensities have been measured as a function of the distance between the nonlinear film and the mirror. The influence of the symmetry of finite laser beams upon the spatial patterns is discussed. The observed patterns are compared with analytically calculated cylindrical modes obtained from a Ginzburg-Landau equation and performing a linear stability analysis. Consideration of finite beam diameters in a first attempt leads to additional boundary conditions for the solutions and the patterns are selected out of a *quasi-discrete* mode spectrum by Talbot-bands instead of a continous spectrum in the plane wave case. It is further shown that the pattern formation in case of axially symmetric input beams is accompanied by O_2 symmetry breaking into spatial structures with D_m symmetry. In case of further symmetry reduction of the system one-dimensional gratings or "rolls", and transitions from rolls

to two-dimensional patterns have been observed. The agreement between theory and experimental observations is good.

Acknowledgements

This work has been financially supported by the Deutsche Forschungsgemeinschaft via the Sonderforschungsbereich 335 "Anisotrope Fluide".

REFERENCES

1. N.B. Abraham, W.J. Firth; *J. Opt. Soc. Am B* **7**, 948 (1990)
2. W.J. Firth, in *Proc. S. Topsøe Summer School Nonlinear Optics*, edited by O. Keller (Nova Science Publ., New York, to appear 1993/94)
3. M. Kreuzer, W. Balzer, T. Tschudi; *Appl. Optics* **29**, 579 (1990)
4. L. A. Lugiato et al.; *J. Opt. Soc. Am B* **7**, 1019 (1990)
5. H. Haken, in *Pattern Formation by Dynamical Systems and Pattern Recognition* edited by H. Haken, Springer Series in Synergetics **5** (Springer, Berlin 1979)
6. T. Kohonen, *Selforganisation and Associative Memory*; Springer Series in Information Sciences **8**, (Springer, Berlin 1989)
7. G.S. McDonald, W.J. Firth; *J. Opt. Soc. Am B* **7**, 1328 (1990)
8. G.D 'Alessandro, W.J. Firth; *Phys. Rev. Lett.* **66**, 2597 (1991)
9. R. Macdonald, H.J. Eichler; *Opt. Commun.* **89**, 289 (1992)
10. M. Tamburrini, M. Bonavita, S. Wabnitz, E. Santamato; *Opt. Lett.* **18**, 855 (1992)
11. I.C. Khoo, S.T. Wu; *Optics and Nonlinear Optics in Liquid Crystals* (World Scientific, Singapore 1992), p.284 f.
12. G. D ' Alessandro, W.J. Firth; *Phys. Rev. A* **46**, 537 (1992)
13. H. Haken; *Synergetics. An Introduction* (Springer, New York 1983)
14. F. W. J. Olver, in *Handbook of Mathematical Functions*, edited by M. Abramowitz, I.A. Stegun (Dover Publ. Inc., New York 1972)
15. R. Macdonald, H. Danlewski; *Preprint*
16. F. Papoff, G. D ' Alessandro, G.-L. Oppo, W.J. Firth; *Phys. Rev. A* **48**, 634 (1993)